

Document downloaded from the institutional repository of the University of Alcalá: <http://dspace.uah.es/>

This is a postprint version of the following published document:

Ramos, M., Vieira, G., de Pablo, M.A., Molina, A., Abramov, A. & Goyanes, G. 2017;2016;, "Recent shallowing of the thaw depth at Crater Lake, Deception Island, Antarctica (2006–2014)", *Catena*, vol. 149, pp. 519-528.

Available at <https://doi.org/10.1016/j.catena.2016.07.019>

© 2016 Elsevier

*(Article begins on next page)*



This work is licensed under a  
Creative Commons Attribution-NonCommercial-NoDerivatives  
4.0 International License.

1           **RECENT SHALLOWING OF THE THAW DEPTH AT CRATER LAKE,**  
2                           **DECEPTION ISLAND, ANTARCTICA (2006 - 2014)**

3           M. Ramos\*<sup>1</sup>, G. Vieira<sup>2</sup>, M.A. de Pablo<sup>3</sup>, A. Molina<sup>3</sup>, A. Abramov<sup>4</sup>, G. Goyanes<sup>5</sup>

4           <sup>1</sup> Department of Physics and Mathematics. University of Alcalá. Madrid, Spain.

5           <sup>2</sup>Centre for Geographical Studies ó IGOT, Universidade de Lisboa, Lisbon, Portugal.

6           <sup>3</sup> Department of Geology, Geography and Environment. University of Alcalá. Madrid, Spain.

7           <sup>4</sup> Russian Academy of Sciences, Institute of Geography. Russia.

8           <sup>5</sup>Instituto de Estudios Andinos óDon Pablo Groeberö (UBA-CONICET). Universidad de Buenos  
9           Aires, Argentina.

10          \*Corresponding author: [miguel.ramos@uah.es](mailto:miguel.ramos@uah.es)

11  
12          **Keywords: Permafrost, Decreasing thaw depth, Active layer, Snow insulation,**  
13          **Antarctic Peninsula.**

14  
15          **ABSTRACT:**

16          The Western Antarctic Peninsula region is one of the hot spots of climate change and  
17          one of the most ecologically sensitive regions of Antarctica, where permafrost is near  
18          its climatic limits. The research was conducted in Deception Island, an active  
19          stratovolcano in the South Shetlands archipelago off the northern tip of the Antarctic  
20          Peninsula. The climate is polar oceanic, with high precipitation and mean annual air  
21          temperatures (MAAT) close to -3 °C. The soils are composed by ashes and pyroclasts  
22          with high porosity and high water content, with ice-rich permafrost at -0.8 °C at the  
23          depth of zero annual amplitude, with an active layer of about 30 cm. Results from thaw  
24          depth, ground temperature and snow cover monitoring at the Crater Lake CALM-S  
25          site over the period 2006 to 2014 are analyzed. Thaw depth (TD) was measured by  
26          mechanical probing once per year in the end of January or early February in a 100 x  
27          100 m with a 10 m spacing grid. The results show a trend for decreasing thaw depth

28 from *ci.* 36 cm in 2006 to 23 cm in 2014, while MAAT, as well as ground temperatures  
29 at the base of the active layer, remained stable. However, the duration of the snow  
30 cover at the CALM-S site, measured through the Snow Pack Factor (SF) showed an  
31 increase from 2006 to 2014, especially with longer lasting snow cover in the spring  
32 and early summer. The negative correlation between SF and the thaw depth supports  
33 the significance of the influence of the increasing snow cover in thaw depth, even with  
34 no trend in the MAAT. The lack of observed ground cooling in the base of the active  
35 layer is probably linked to the high ice/water content at the transient layer. The  
36 pyroclastic soils of Deception Island, with high porosity, are key to the shallow active  
37 layer depths, when compared to other sites in the Western Antarctic Peninsula (WAP).  
38 These findings support the lack of linearity between atmospheric warming and  
39 permafrost warming and induce an extra complexity to the understanding of the effects  
40 of climate change in the ice-free areas of the WAP, especially in scenarios with  
41 increased precipitation as snow fall.

42

## 43 **1. INTRODUCTION**

44 Deception Island is located in the South Shetlands archipelago, north of the Antarctic  
45 Peninsula (AP), one of Earth's regions with strongest atmospheric warming signal,  
46 with an increase of *ci.* 3°C in the MAAT from the 1950s (Marshall et al., 2002;  
47 Meredith and King, 2005; Turner et al., 2005; Turner et al., 2009; Turner et al., 2013).  
48 The environmental consequences of this warming on glaciers and ice-shelves have  
49 been widely studied, but the consequences for permafrost, are only now beginning to  
50 be investigated (Vieira et al., 2010; Bockheim et al., 2013). Permafrost temperature  
51 and active layer thickness (ALT) are Essential Climate Variables as defined by the  
52 Global Climate Observing System (GCOS/WMO) (Smith and Brown, 2009., Bojinski

53 et. al., 2014) and are key indicators of climate change in the Polar Regions (Anisimov  
54 et al., 1997; Burgess et al., 2000), reflecting changes in the ground surface energy  
55 balance (World Meteorological Organization, 1997). The distribution and properties  
56 of permafrost and the ALT in the Antarctic Peninsula region are poorly understood  
57 (Bockheim, 1995; Bockheim et al., 2013). The situation started to change with the  
58 International Polar Year (IPY) 2007-2008, which was the framework for an  
59 international effort to improve monitoring of permafrost and the ALT across the  
60 Antarctic (Vieira et al., 2010).

61 The Circumpolar Active Layer Monitoring (CALM) program is a network of  
62 permafrost observatories distributed over both Polar Regions and selected mid-latitude  
63 mountain ranges (Brown et al., 2000). CALM is an international global-change  
64 monitoring program concerned with ALT dynamics and the shallow permafrost  
65 environment, with CALM sites in the Southern Hemisphere designated as CALM-S  
66 (Guglielmin, 2006; Nelson and Shiklomanov, 2010). CALM-S sites are also integrated  
67 in the Global Terrestrial Network for Permafrost (GTN-P, WMO/GCOS) (Burgess et  
68 al., 2000).

69 Low altitude permafrost temperatures are slightly below 0°C in the South Shetlands,  
70 showing that the region is near its climatic boundary, thus being probably one of the  
71 regions with highest sensitivity to climate change in the Antarctic (Ramos et al., 2007;  
72 Ramos and Vieira, 2009; Bockheim et al., 2013). This fact reinforces the importance  
73 to study the evolution of permafrost and active layer in the region.

74 The CALM-S protocol as an approach to standardize ALT monitoring has been  
75 implemented by our team in Deception Island, one of the scarce areas of the South  
76 Shetlands allowing using mechanical probing to measure thaw depth. Despite being  
77 an active volcano, the high interstitial ice-content of permafrost and high porosity

78 volcanoclastic soils, favour thermal insulation and permafrost is ubiquitous almost  
79 down to sea-level. Geothermal anomalies show only very local effects, mainly along  
80 faults and within buffers a few hundred meters wide (Goyanes et al., 2014). Therefore,  
81 the ALT conditions in most of the island are not affected by the geothermal heat flux.  
82 CALM-S monitoring sites target at identifying the spatial variability of the ALT and  
83 the controlling effects of parameters such as topography, soil physics properties,  
84 vegetation, hydrology and snow cover. Observations are usually carried out in a 100 x  
85 100 m grid with sampling nodes at 10 m spacing, where TD is measured by mechanical  
86 probing close to the end of the thaw season. In complex topography sites, smaller grids  
87 may be implemented. Arrays of shallow boreholes for monitoring ground temperatures  
88 may also be used in areas where probing is not possible and a meteorological station  
89 is used to analyze the climate conditions. At some Antarctic sites, this approach is  
90 complemented with deeper boreholes that are monitored for permafrost temperatures  
91 (Vieira et al., 2010).

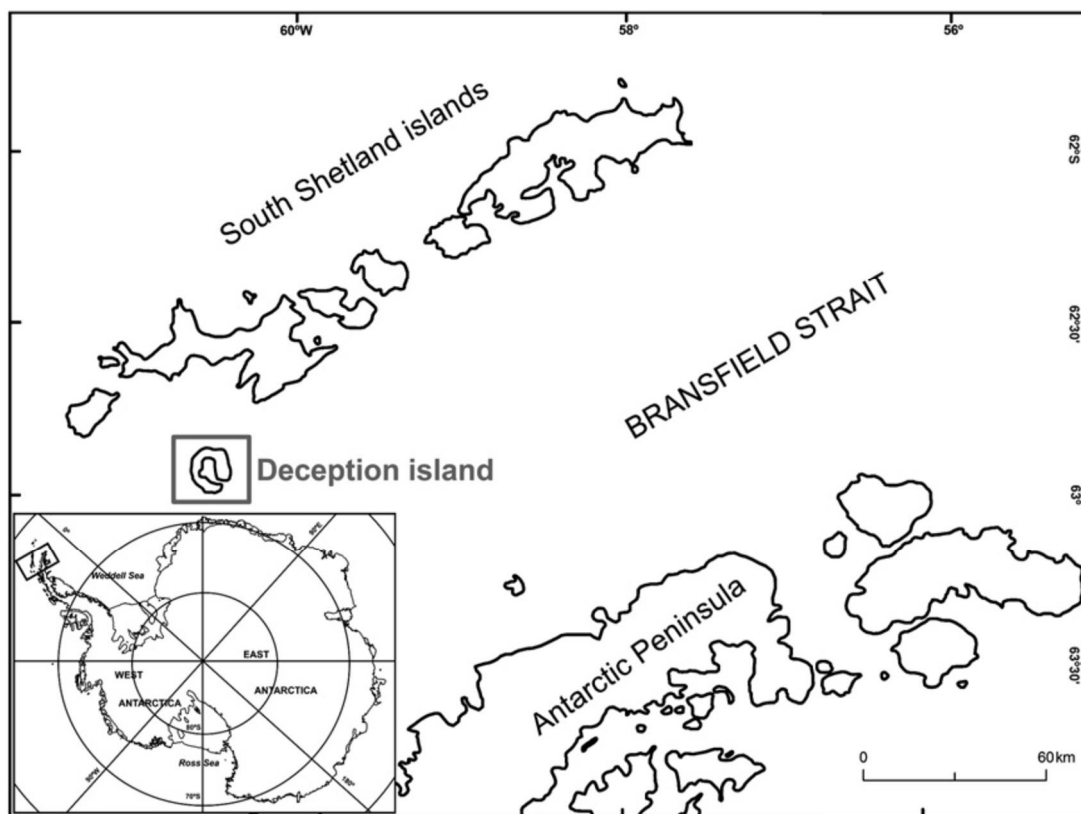
92 This paper aims at characterizing the active layer thermal regime and climate controls,  
93 through the analysis of thaw depth (TD), air and ground temperatures and snow cover  
94 observations at the Crater Lake CALM-S site in Deception Island using data from 2006  
95 to 2014.

96

## 97 **2. STUDY AREA**

98 Deception Island (62° 55 S, 60° 37 W) is located in the South Shetlands archipelago  
99 in the Bransfield Strait, about 100 km north of the Antarctic Peninsula (AP) (figure 1).  
100 The horseshoe shaped island is a stratovolcano with a diameter of 15 km, a maximum  
101 elevation of 539 m asl at Mount Pond in the eastern part of the volcano rim and with

102 a 7 km wide caldera open to the sea. About 57% of the island is covered by glaciers  
103 and an area of about 47 km<sup>2</sup> is glacier free (Smellie and López-Martínez., 2002).



104  
105 Figure 1.-Location of Deception Island in the South Shetlands Archipelago (Antarctica).

106 The climate of the South Shetlands is cold-oceanic with frequent summer rainfalls and  
107 a moderate annual temperature range. MAAT are close to -3 °C at sea level and average  
108 relative humidity is very high, ranging from 80 to 90%. The weather conditions are  
109 dominated by the influence of the polar frontal systems, and atmospheric circulation  
110 is variable, with the possibility of winter rainfall (Styszynska., 2004). The annual  
111 meteorological data describe two seasons corresponding to the annual cycle of soil  
112 freezing and thawing (Ramos et al., 2012). Electrical resistivity surveying suggests  
113 permafrost thickness to be between 3 and 25 m in Deception Island (Vieira et al.  
114 2008b; Bockheim et al., 2013; Goyanes et al., 2014).

115 As a result of recent eruptions, Deception Island is covered by volcanic ash and  
116 pyroclasts, and many of the glaciers remain ash-covered today. Pyroclastic deposits

117 covered the snow mantle, and buried snow is still present at some sites. Deposits are  
118 very porous and insulating with high water/ice content near the surface, and give rise  
119 to a thin ALT, varying from 10 to 96 cm depth (Bockheim et al., 2013). On lower  
120 valley slopes, exposures of fossil snow (buried ice) with perennially frozen ice-  
121 cemented volcanic debris on top can be observed, testifying post-eruption aggradation  
122 of permafrost. At these sites, ice-cemented permafrost also occurs under the buried-  
123 ice layer. Buried-ice is widespread on Deception Island, especially along the lower  
124 slopes, and ice-cemented permafrost occurs almost down to sea level as shown by  
125 geophysical surveying and trenches (Vieira et al., 2008b).

126 The Crater Lake CALM-S site is located in a small and relatively flat plateau-like step  
127 covered by volcanic and pyroclastic sediments at 85 m a.s.l north of Crater Lake  
128 ( $62^{\circ}59'06.7''$ S,  $60^{\circ}40'44.8''$ W). The site was selected due to its flat characteristics,  
129 absent summer snow cover, distance to known geothermal anomalies, good exposure  
130 to the regional climate conditions (mitigating site specific effects and being  
131 representative in a regional context) and also because of its proximity to the Spanish  
132 station "Gabriel de Castilla". The ground surface is completely devoid of vegetation  
133 and the MAAT at the Crater Lake CALM-S site between 28/01/2009 to 22/01/2014  
134 was  $-3.0^{\circ}\text{C}$ .

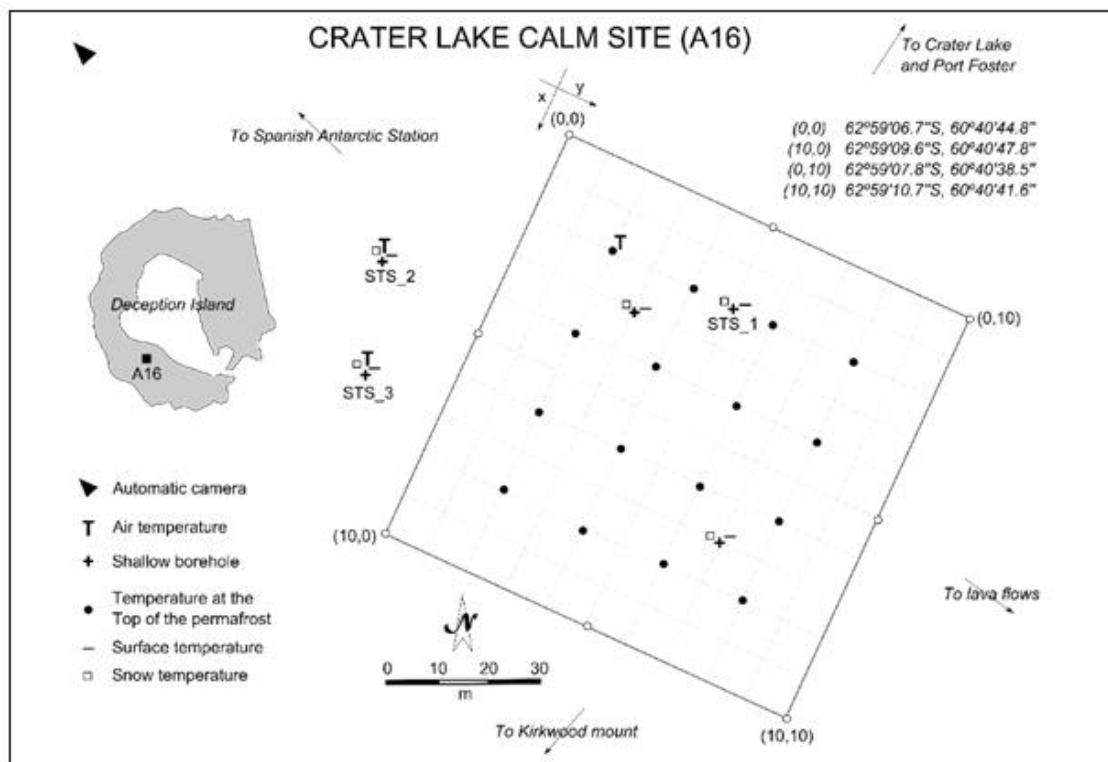
135 Borehole temperature data show warm permafrost ( $-0.3^{\circ}\text{C}$  to  $-0.9^{\circ}\text{C}$ ), with thickness  
136 varying between 2.5 and 5.0 m (Vieira et al., 2008a; Ramos et al., 2010). The ALT  
137 derived from the borehole temperature profiles from 2010 to 2013 varied from 30 to  
138 40 cm.

139

### 140 **3. MATERIALS and METHODS**

#### 141 **3.1 Observational setting**

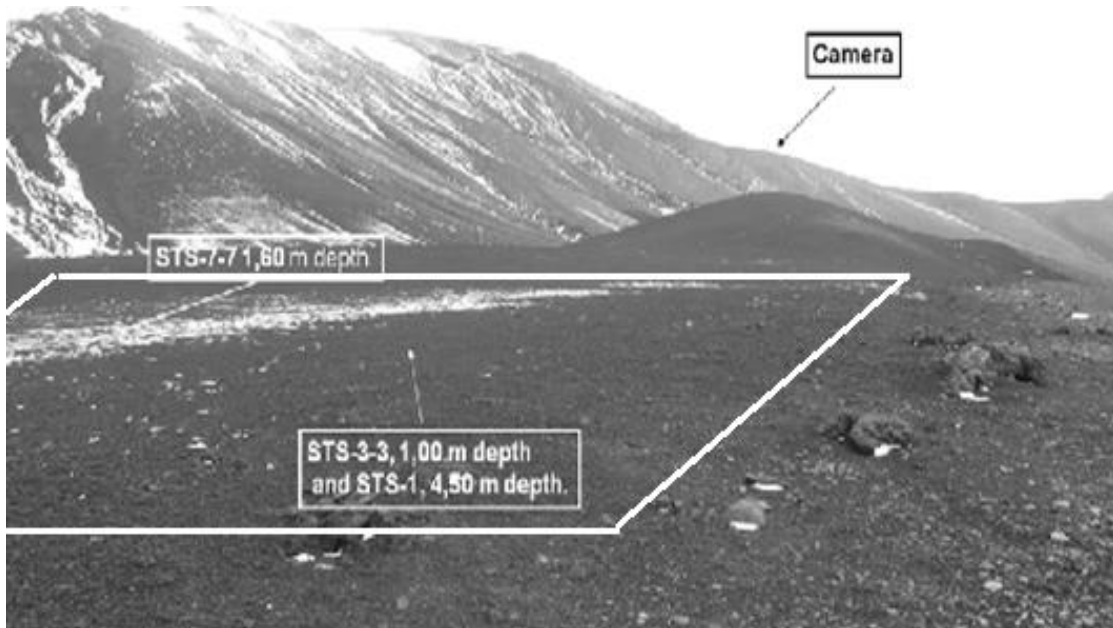
142 The Crater Lake CALM-S site consists of a 100×100 m grid with 121 nodes spaced at  
 143 10 m intervals and was installed in January 2006 (figures 2 and 3). Thaw depth (TD)  
 144 is measured manually by mechanical probing (1-2 cm accuracy) once per year in late  
 145 January or early February (coinciding with the end of summer), depending on  
 146 logistical constraints since the research station is only open during the summer season  
 147 (Ramos et al., 2007).



148  
 149 Figure 2. Instrumentation setting at the Crater Lake CALM-S site.

150 Since the installation of the CALM-S, the observational system has been continuously





151

152 Figure 3.-General view of the Crater Lake CALM-S site, the arrows point the position of  
 153 the camera (up right) and boreholes (center).

154 improved and the following parameters are currently monitored (tables 1 and 2):

- 155 - Air temperatures at 1.60 m above the surface, monitored hourly since 2009.
- 156 - Ground temperatures in shallow boreholes down to 1.00 m (node 3, 3), 1.60 m  
 157 (node 7,7) and 4.50 m (node 2,5) (figure 3). The boreholes have a diameter of 32  
 158 mm, are cased with PVC pipes, air-filled and temperatures are measured with  
 159 ibuttons (see table 2 for specifications) at different depths starting at 2.5 cm.
- 160 - Ground temperatures in 16 very shallow boreholes regularly distributed in the grid,  
 161 with a single ibutton close to the base of the active layer (TBAL) at 40 cm depth  
 162 (table 2).
- 163 - Snow thickness estimated using near surface air temperature miniloggers installed in  
 164 a stake (5, 10, 20, 40, 80 cm) and a Campbell CC640 time-lapse camera with daily  
 165 pictures at 11:00, 12:00 and 13:00 (local solar time). This approach allows evaluating  
 166 the snow distribution.

Coordinates (node 0, 0)	Average altitude (m a.s.l.)	Snow-stakes: snow temperature array and mini array	Air Temperature	Boreholes	Time lapse camera
62°59'06.7" S 60°40'44.8" W	85	2 nodes (3,3) (7,7)	1 node (2,2)	4.50 m node (2,5) 1.00 m node (3,3) 1.60 m node (7,7)	1

167 Table 1.-Crater Lakeö CALM-S site instrumentation position.

	Node	Sensor type	Accuracy (°C)	Resolution (°C)	Sampling rate (h)	Sensor Position (cm)
Air temperature	(2,2)	Pt-100, Tinytag	0.2	0.05	1	160 (height)
Borehole (4.50 m)	(2,2)	Ibutton DS1922L	0.5	0.06	3	5, 10, 20, 40, 80, 120, 160, 200, 250, 300, 350, 400, 450 (depth)
Borehole (1 m)	(3,3)	Ibutton DS1922L	0.5	0.06	3	2.5, 5, 10, 20, 40, 70, 100 (depth)
Borehole (1.6 m)	(7,7)	Ibutton DS1922L	0.5	0.06	3	2.5, 5, 10, 20, 40, 70, 100, 150 (depth)
Temperature close to the base of the active layer	(2-8, 2-8) at 20 m interval (16 nodes)	Ibutton DS1921G	1	0.5	3 or 4	40 (depth)
Snow stakes	(3,3), (7,7)	Ibutton DS1921G	1	0.5	3	5, 10, 20, 40, 80 (height)

168 Table 2. Crater Lake CALM-S site instrumentation details.

169 3.2 Estimation of snow thickness

170 In order to estimate snow thickness, near-surface temperatures acquired by an array of  
171 sensors installed along a 1.60 m long stake, were analyzed. The method implemented

172 by Lewkowicz and Bonnaventure (2008) and based on the changes in thermal regime  
173 along the stake when sensors are inside the snow pack, was used.

174 The daily snow thickness ( $x_i$ ) was classified according to the following levels:  $x_1 \leq$   
175 10 cm,  $10\text{cm} < x_2 \leq 20$  cm,  $20\text{cm} < x_3 \leq 40$  cm, considering that the periods of snowpack  
176 persistence for each level are ( $t_1, t_2$  and  $t_3$ ). The Mean Snow Layer Thickness (MSLT)  
177 for the entire snow cover period ( $t = t_1 + t_2 + t_3$ ) for each of the snow stakes was calculated  
178 using the following equation (1).

179

$$180 \quad MSLT(node) = \frac{[t_1(node) \times 0,1 + t_2(node) \times 0,2 + t_3(node) \times 0,4]}{\sum_i t_i} (m) \quad (1)$$

181

182 The mean snow pack factor (SF) aims at assessing an annual average of snow  
183 distribution over the CALM-S grid and is an average of the MSLT at both snow stakes  
184 (equation 1).

185

$$186 \quad SF = \frac{MSLT(3,3) + MSLT(7,7)}{2} (m) \quad (2)$$

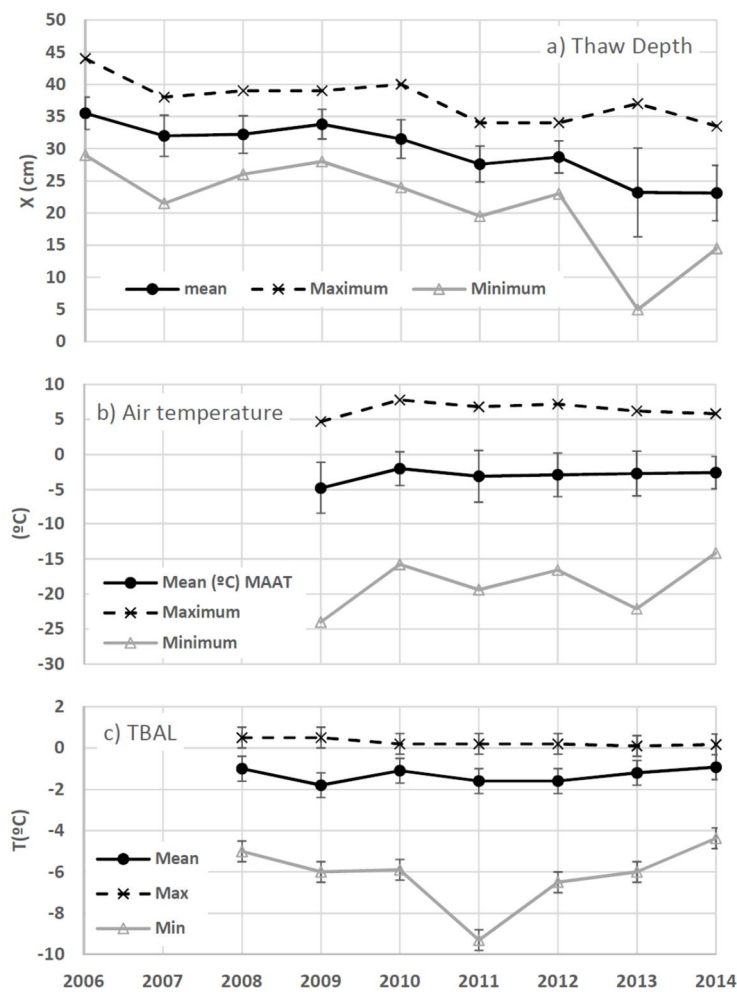
187

## 188 **4. RESULTS**

### 189 **4.1 Active layer**

190 Figure 4a shows the evolution of thaw depth (TD) at the Crater Lake CALM-S grid  
191 from 2006 to 2014. The mean TD for the 121 nodes for the whole period was 29.7 cm,  
192 but the nine year time series shows a decreasing average TD from 35.5 cm in 2006 to  
193 23.1 cm in 2014. Although not constant, with minor increases in TD in 2009 and 2012,  
194 the trend is noticeable and followed with higher irregularity by the local maxima and  
195 minima measured in individual nodes. Figure 5 shows the spatial distribution of TD as

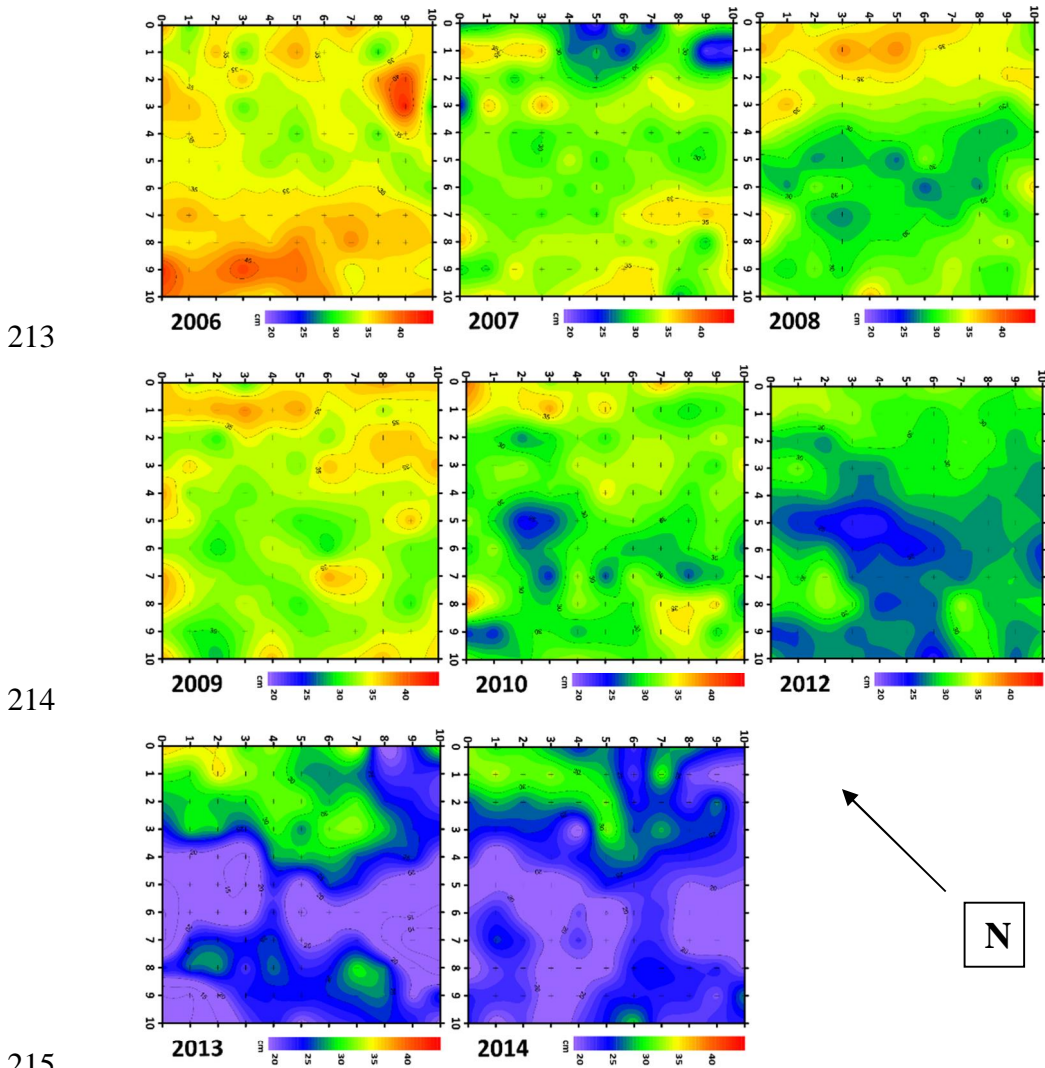
196 measured in the grid nodes along the study period. The increasing trend observed in  
 197 the average values is also clear in the spatial patterns of thaw.  
 198 Figure 4b shows the evolution of the air temperatures at the study site from 2009 to  
 199 2014. Mean annual air temperature was very stable around -3 °C, the same happening  
 200 with absolute maxima and minima. The extreme records were +7.8 °C in 2010 and -  
 201 24.0 °C in 2009.



202  
 203 Figure 4. Thaw depth and temperatures at the Crater Lake CALM-S site from 2006 to  
 204 2014. a. Thaw depth, b) Air temperatures, c) Temperature at the bottom of the active layer  
 205 (40 cm - TBAL).

206 The mean ground temperature close to the base of active layer (TBAL) in the 16 very  
 207 shallow boreholes from 2008 to 2013 was -1.3 °C, with minor interannual changes and  
 208 no appreciable trend. The mean maxima were slightly above 0 °C, showing an annual

209 extreme value of 0.5 °C (2008 and 2009) and the minima were always below -4 °C,  
210 down to -9.3 °C in 2011. Accounting for the instrumental errors of the monitoring  
211 devices, the maxima was therefore always close to the water melting point in normal  
212 conditions.



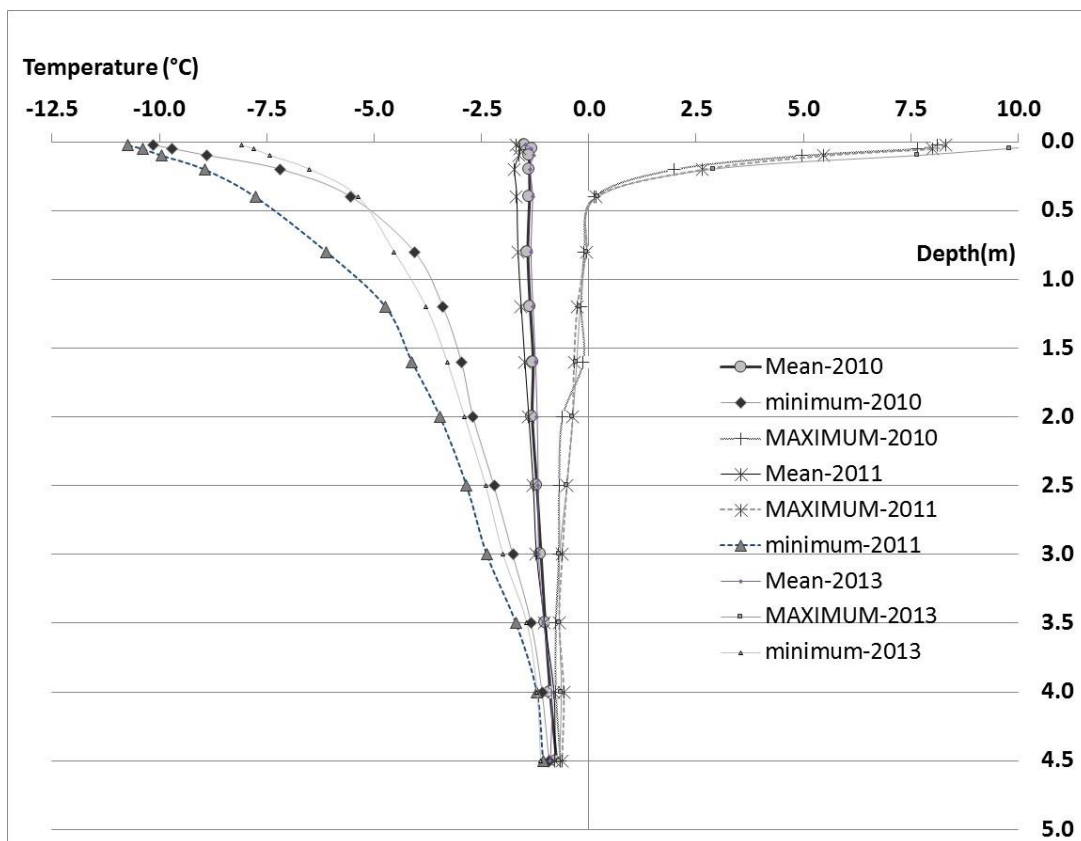
216 Figure 5. Summer thaw depth from 2006 to 2014 at the Crater Lake CALM-S site. Scale  
217 in decameters.

218

#### 219 4.2 Permafrost

220 The borehole temperatures from 2010 to 2013 show that the maximum active layer  
221 thickness (ALT) calculated using the 0 °C isotherm was 0.40 m with an isothermal  
222 transition in the range of 0.4 to 1.2 m, and the mean annual ground surface temperature,

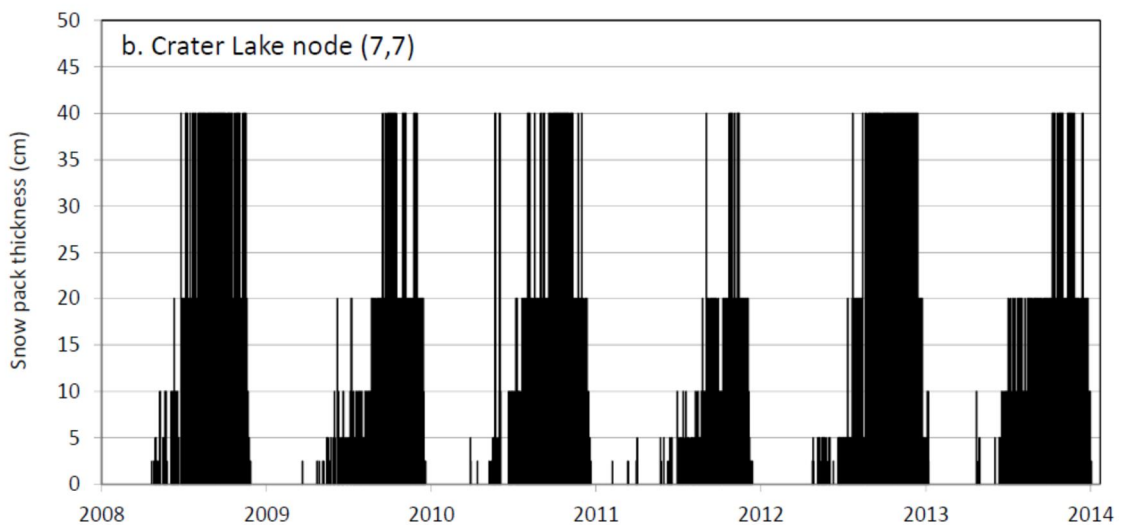
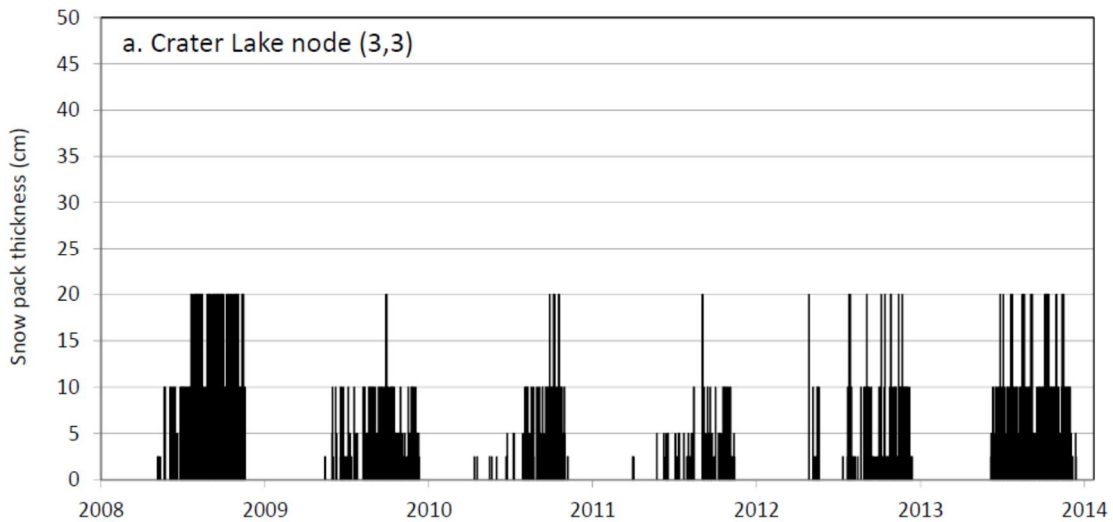
223 at 2,5 cm depth was -1.7 °C, showing an annual extreme value of 10.7 °C (2013) and  
 224 the minima were always below -8.1 °C, down to -16.0 °C in 2012. The depth of zero  
 225 annual amplitude should be slightly below the bottom of the borehole, just below 4.50  
 226 m, with a temperature of ci. -0.9 °C. Figure 6 shows the thermal envelope for 2010 to  
 227 2013 (2012 is not represented due to the data series is not competed).  
 228



229  
 230 Figure 6.-Temperature distribution into the borehole STS-1 (node 2, 5) in the Crater  
 231 Lakeö CALM-S site. Maximum, minimum and mean annual ground temperatures at  
 232 different depth are represented (2010, 2011 and 2013, 2012 is not represented because is  
 233 not complete the data serie).

234 **4.3 Average snow pack**

235 The dataset measured by the snow stake installed in the nodes (3,3) and (7,7),  
236 complemented with the pictures taken by the digital camera, allowed characterizing  
237 the evolution of the snow pack from 2008 to 2013 (figure 7).



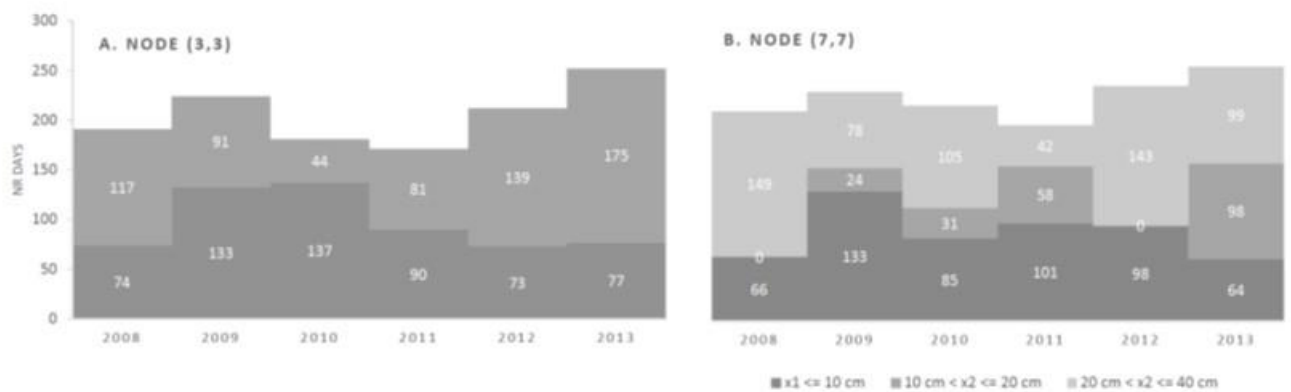
240 Figure 7. Snow pack thickness at the Crater Lake CALM-S site from 2008 to 2013. a)  
241 node (3,3), b) node (7,7).

242 If we account for the number of days of snow pack duration ( $t_i$ ) below the identified  
243 threshold thicknesses ( $x_1 \leq 10\text{cm}$ ,  $10\text{cm} < x_2 \leq 20\text{cm}$ ,  $20\text{cm} < x_3 \leq 40\text{cm}$ ), the maximum  
244 value of  $t_1$  occurred in 2010 (137 days) at node (3,3) and the minimum occurred in

245 2008 (66 days) at node (7,7) (figures 8a, b). The number of days with less than 20 cm  
 246 of snow cover ( $t_2$ ) showed a maximum of 175 days in 2013 in node (3,3), while the  
 247 threshold 40 cm was only attained at node (7,7).

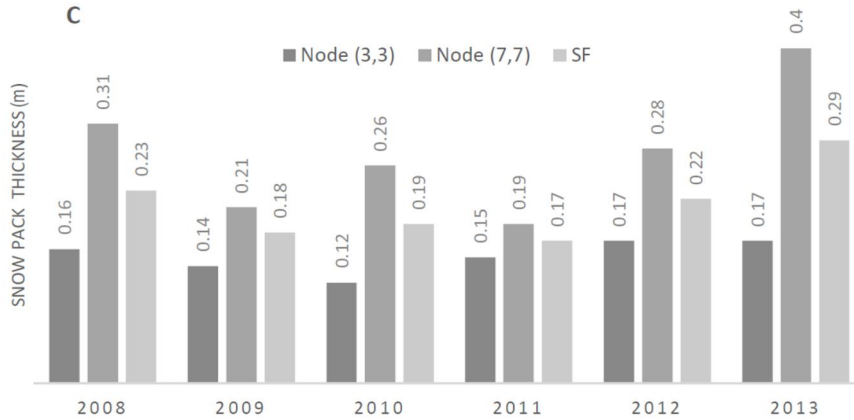
248 Node (7,7) showed an earlier snow pack setting and later melt, resulting in longer  
 249 lasting snow pack every year. The snow thickness frequently reached over 40 cm at  
 250 node (7,7), but never in (3,3). In the later, snow was generally 10-20 cm thick, but  
 251 rarely passed 20 cm. In node (7,7), the snow thickness showed very frequently 20 to  
 252 40 cm. The snow pack generally settled around mid-April to May and lasted until mid-  
 253 November to December eve first January, with a significant delay in the melt date in  
 254 the more recent years.

255 The results from equations (1) and (2) are shown in figure 8c. The larger values of SF  
 256 occurred in 2013 (29 cm) and 2008 (23 cm), and the lower in 2011 (17 cm) and 2009  
 257 (18 cm).



258





259

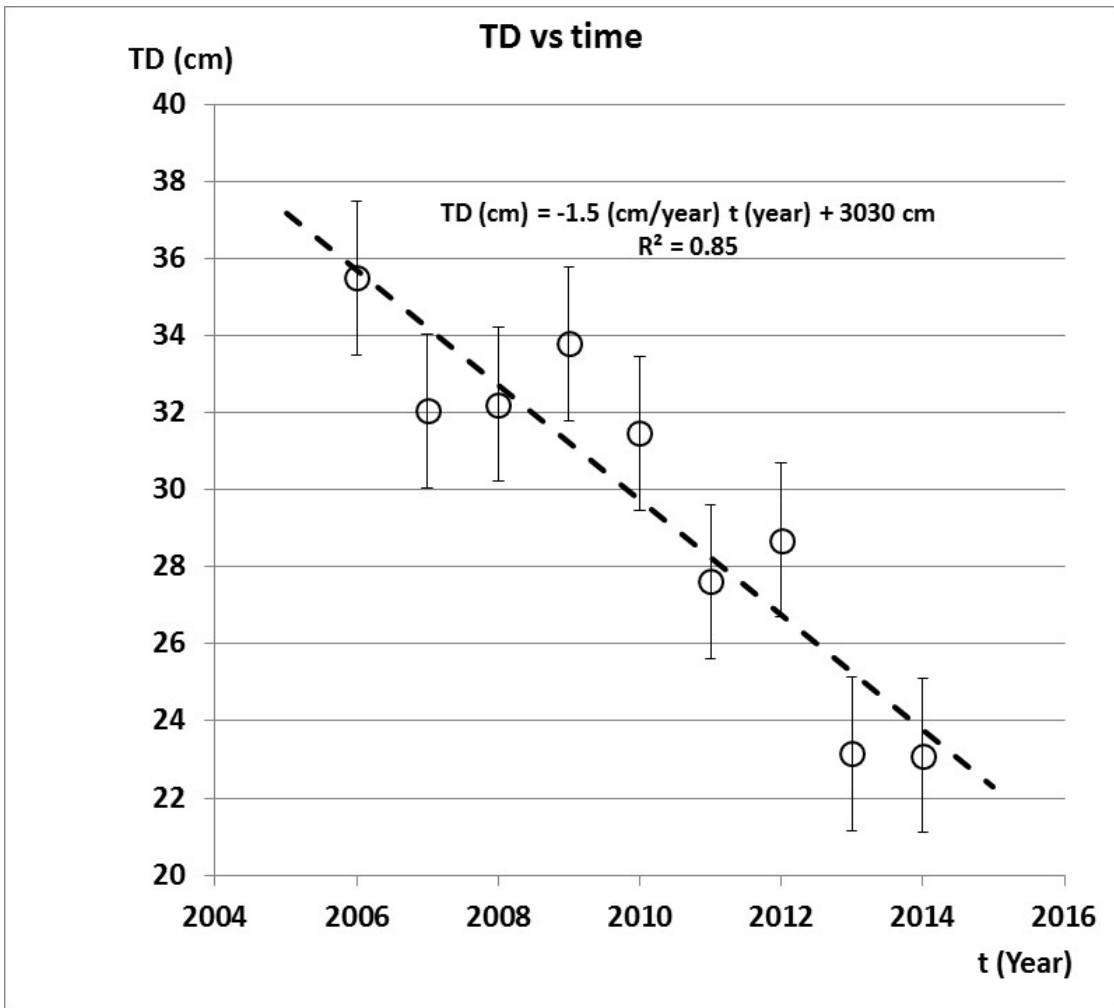
260 Figure 8. Characteristics of the snow pack at the Crater Lake CALM-S site from 2008 to  
 261 2013. a) Snow pack persistence ( $t_i$ - days) at node (3,3), b) snow pack persistence in node  
 262 (7,7), c) Snow pack thickness and Snow Pack Factor (SF).

263

## 264 5. DISCUSSION

### 265 5.1 Thaw depth

266 The analysis of the spatial distribution of thaw depth across the crater lake CALM-S  
 267 site (figure 5) shows that the area with small values corresponds to sectors which are  
 268 less wind-exposed and with lower relief, showing also a longer and more stable snow  
 269 cover. This is also shown in the longer lasting and thicker snow pack in node (7,7)  
 270 than in (3,3) (figures 7 and 8).



271

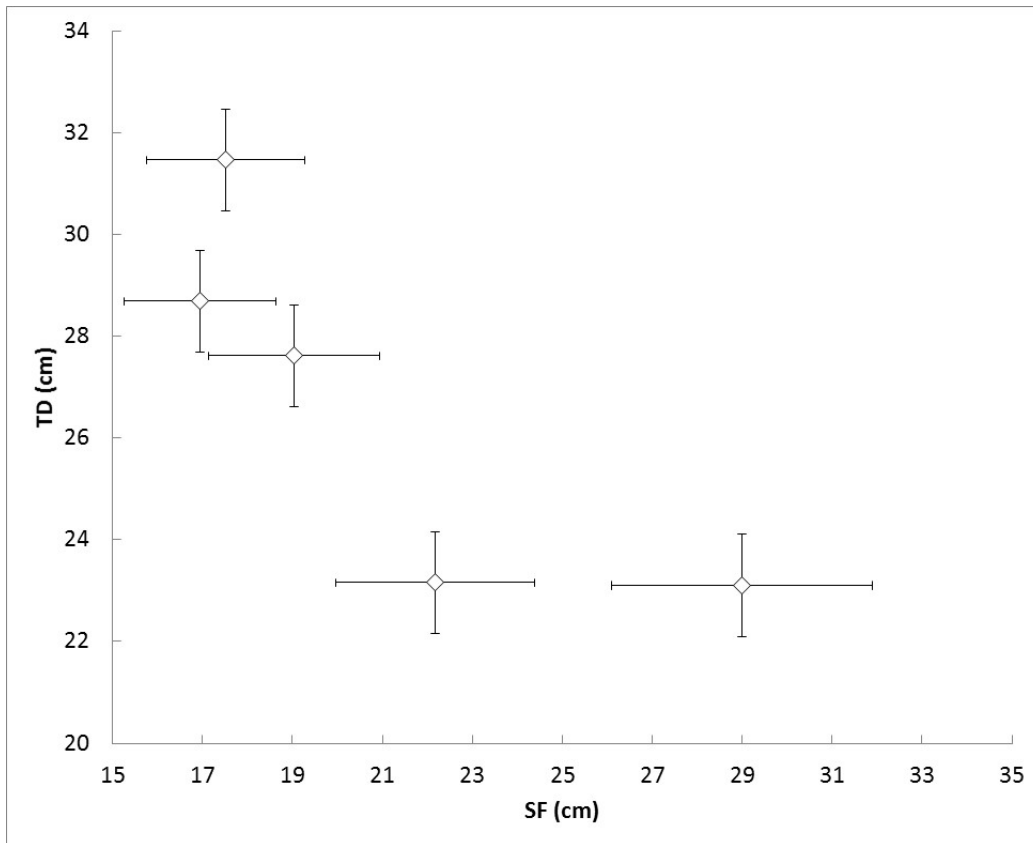
272 Figure 9. Summer mean thaw depth in Crater Lake CALM-S from 2006 to 2014.

273 Despite a slight interannual variability, the decreasing trend in thaw depth between  
 274 2006 ( $35.5 \pm 2$  cm) and 2014 ( $23.1 \pm 2$  cm) shows a statistically significant coefficient  
 275 of correlation of 0.85 (figure 9). This trend is consistent with the deceleration in the  
 276 glacial retreat identified in Livingston Island by Navarro et al. (2013) and may be also  
 277 related to an increase of snow precipitation pointed by Osmanoglu et al. (2014). The  
 278 impacts of increased snow thickness on a decreasing active layer depth have also been  
 279 shown by Jiménez et al. (2014) that study the thermal behaviour of the active layer by  
 280 mean of the enthalpy model in function of the snow cover near to the Hurd peninsula  
 281 in Livingston Island, showing a reduction of the soil surface energy balance when  
 282 increasing the snow layer thickness. In Byers Peninsula (Livingston Island), De Pablo

283 et al. (2016) study the evolution of the snow cover at the Limnopolar Lake CALM-S  
284 site and conclude that the evolution of the snow cover during the 2009-2014 period  
285 resulted on about similar snow depths, with annual mean values of about 45 cm. The  
286 snow onset remained about constant with small variations of 10 days in early March,  
287 but the snow offset had significant variations, increasing in the last three years for  
288 more than 60 days. Therefore, the main conclusion that they extract from these data is  
289 that the increase in the snow duration is resulting in the reduction of the thaw period  
290 in the ground. In the same place Byers Peninsula but in three different monitoring sites  
291 with specific geomorphological characteristics Oliva et al. (2016) extrapolated the  
292 presence of stable frozen layer conditions in the range of 85 to 155 cm, these depths  
293 are close to the 1.3 m reported for the depth of the permafrost table at the nearby  
294 Limnopolar site by de Pablo et al. (2014).

295 In other localities of the Antarctic Peninsula region, the ALT showed also a high  
296 variability, such as on Signy Island where ALT was influenced by vegetation and  
297 ranged between 0.8 to 1.8 m (Guglielmin et al., 2012), or in conditions with colder  
298 climate on James Ross Island where the ALT reached 0.5 to 0.8 m at sites with  
299 different lithological properties (Hrbáček et al., in press)

300 In our study site in Deception Island the influence of the snow pack on the mean annual  
301 thaw depth is well represented by SF through a negative correlation, showing that the  
302 increase of snow layer thickness and its persistence period causes a decrease of the  
303 maximum thaw depth, as shown in figure 10.



304

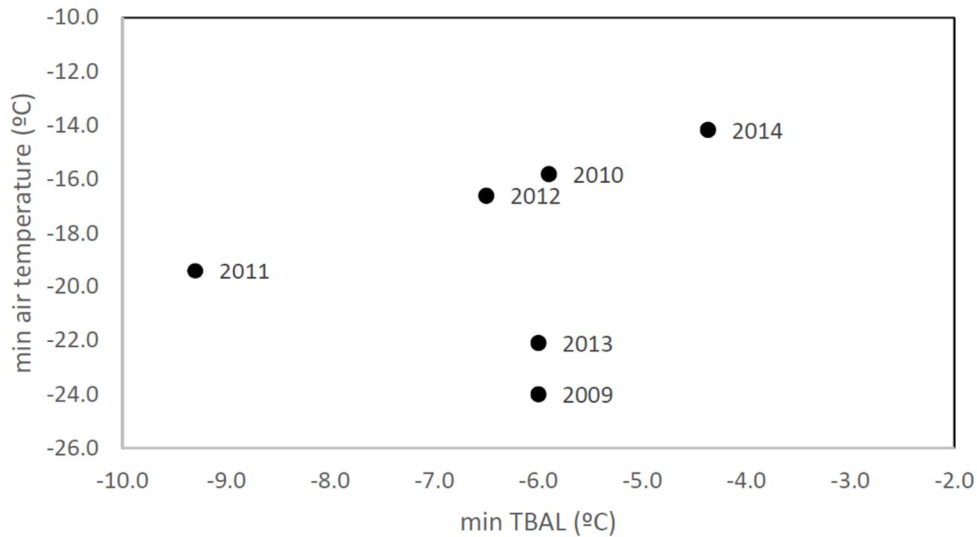
305 Figure 10. Maximum thaw depth (TD) as function of the Snow factor (SF) for the  
 306 Crater Lake CALM-S site between 2008 and 2013.

307

308 **5.2 Temperature close to the base of the active layer**

309 The mean temperature close to the base of the active layer (TBAL) was stable during  
 310 the whole study period (figure 4c). During winter and spring, the snow cover  
 311 influences significantly TBAL. Figure 11 shows that the years with less days of snow  
 312 cover (2010, 2011, 2012 and 2014) present a good linear fit between the minimum  
 313 annual air temperature and TBAL, implying a poor thermal insulation of the snow  
 314 pack. On the other hand, the two years with longer snow pack duration (2009 and  
 315 2013), plot clearly outside the best fit.

316



317

318 Figure 11. Minimum temperature close to the base of the active layer (TBAL) versus  
 319 minimum air temperature from 2009 to 2014.

320 It is also worth comparing 2009 and 2011. The former showed an air temperature  
 321 minimum of -24.0 °C and a minimum TBAL of -6.0 °C, while the later, showed higher  
 322 minima (-19.4 °C), but a lower minimum TBAL (-9.3 °C). In this case, SF was very  
 323 similar in both years (18 and 17 cm), but snow cover settled one month earlier and  
 324 more homogeneously in 2009 (15/04/2009) than in 2011 (18/05/2011), which  
 325 generated a stronger thermal insulation in the former. This effect seems to have  
 326 contributed to the largest TD in the summer of 2010 (31.5 cm), when compared to the  
 327 summer of 2012 (28.7 cm).

328 The annual maxima of TBAL were stable, within  $0.0 \pm 0.5$  °C due to the damping  
 329 effect caused by latent heat fluxes on top of the ice-rich permafrost during the thaw  
 330 season.

331

### 332 5.3 Permafrost temperatures

333 Maximum annual ground temperatures show similar values and active layer depth of  
 334 approximately 0.4 m at Crater Lake CALM-S in the 4 years with data. Figure 6 shows

335 a typical permafrost temperature profile into the borehole STS-1 node (2, 5) at Crater  
336 Lake, with maximum summer temperatures nearly isothermal at about 0 °C from 0.4  
337 to 1.2 m depth. This temperature profile reflects the influence of the ice rich  
338 permafrost, as well as of the saturated layer just above the permafrost table, which  
339 mitigate ground warming. The small interannual range in the maximum mean  
340 temperatures for the shallower sensor (2.5 cm depth) at the different years, varying  
341 from 8.1 °C in 2010 to 10.7 °C in 2013 is due to the absence of snow during the  
342 summer, small interannual air temperature range with similar maxima and latent heat  
343 effects due to the high moisture content of the ground.

344 However, the ground temperature minima in this shallow depth (2.5 cm) are very  
345 variable inter-annually, with values from -8.1 °C in 2013 to -16.0°C in 2012, reflecting  
346 a strong influence from snow cover variability and differences in winter air  
347 temperatures.

348 The mean annual ground temperatures vary very slightly with depth (ci. 1.1 °C).  
349 MGST is  $-1.7 \pm 0.5$  °C which corresponds to a thermal offset of about 0.8 °C.

350

#### 351 **5.4 Average snow pack**

352 Snow pack thickness data shows that snow settles between 2 and 4 weeks earlier at  
353 node (7,7) than (3,3), which is at a more convex site and closest to the interfluve (figure  
354 5 and 8). A similar effect occurs at snow melt, with the ground becoming snow free  
355 about a week later at node (7,7). This results in an average of more 27 days per year  
356 of snow cover difference between the nodes (3,3) and (7,7). MSLT values are also  
357 higher at (7,7) (25 cm vs 15 cm), reflecting the wind sheltered position of that part of  
358 the CALM-S site (figure 8c). These spatial differences also affect the spatial  
359 distribution of TD (figure 5).

360 **6. CONCLUSIONS**

361 Ground temperature observations from the Crater Lake CALM-S site show that  
362 permafrost is warm, with temperatures close to  $-0.9\text{ }^{\circ}\text{C}$ , with an active layer depth of ci.  
363 40 cm and a thermal offset of  $0.8\text{ }^{\circ}\text{C}$ . The zero annual temperature depth is shallow and  
364 should be just below 4.5 m depth in contrast to other sites in the Western Antarctic  
365 Peninsula in high diffusivity bedrock settings (Ramos et al., 2009; Bockheim et al., 2013;  
366 Guglielmin, et al., 2014). These characteristics are strongly influenced by the high  
367 porosity pyroclastic debris of Deception Island, which show a high ice-content at the base  
368 of the active layer.

369 Contrary to what would be expected given the general warming signal of the Western  
370 Antarctic Peninsula during the last decades, the thaw depth measured during the summer  
371 at the Crater Lake CALM-S site showed an approximately linear decreasing trend from  
372 2006 to 2014 at a rate of about 1.5 cm/year. The mean annual air temperatures from 2008  
373 to 2014 were relatively stable at ci  $-3\text{ }^{\circ}\text{C}$ , therefore showing no clear control on the active  
374 layer thinning. The temperatures at 40 cm depth also showed no trend during the same  
375 period, which means that the thinning was not due to increase MAAT and also did not  
376 resulted in a cooling at shallow depth. The main factor controlling the decreasing thaw  
377 depth was snow cover, with increased duration, especially during the spring and early  
378 summer, thus insulating the ground from warming. The reason for this phenomena not  
379 having been accompanied by ground cooling is probably related to the high moisture  
380 content and ice-rich permafrost in the transient layer, which mitigate temperature change.  
381 The results presented in this paper are limited to a small number of years but this is one  
382 of the longest data series on thaw depth from an Antarctic CALM-S. The results should  
383 be interpreted with caution, but they support the fact that permafrost and active layer  
384 dynamics in the Maritime Antarctic is complex and cannot be directly linked to

385 atmospheric warming alone. The changing snow cover plays a major role in the ground  
386 thermal regime and on permafrost and it needs to be better assessed, especially since  
387 regional models indicate an increase in precipitation following atmospheric warming and  
388 winter sea ice losses in the Western Antarctic Peninsula.

389

### 390 **Acknowledgements**

391 Authors thank to the Spanish Polar Program, Unit of Marine Technology from Spanish  
392 National Research Council, as well as to the Spanish Army and Spanish Navy crews  
393 involved on Antarctic Campaigns for made possible the continuous data acquisition. Our  
394 special thanks to ðGabriel de Castillaö Spanish Antarctic Station. This research was  
395 possible thanks to financial support of PERMATHERMAL, PERMASNOW (CTM2014-  
396 50521-R), ANTARPERMA (CTM2011-15565-E), and PERMAPLANET (CTM2009-  
397 10165) research projects from the Spanish National Research Program.

398

### 399 **REFERENCES:**

400 Anisimov, O.A., Shiklomanov, N.I., Nelson, F.E., 1997. Global warming and active  
401 layer thickness: results from transient general circulation models. *Global and Planetary*  
402 *Change* 15, 61677. (ISSN: 0921-8181).

403

404 Bockheim, J.G., 1995. Permafrost distribution in the Southern Circumpolar Region  
405 and its relation to the environment: a review and recommendations for further research.  
406 *Permafrost and Periglacial Processes* 6, 27645.

407

408 Bockheim, J., Vieira, G., Ramos M., López-Martínez, J., Serrano, E., Guglielmin, M  
409 Wilhelm, K., Nieuwendam, A., 2013. Climate warming and permafrost dynamics in



410 the Antarctic Peninsula region. *Global and Planetary Change* 100. 2156223.  
411 <http://dx.doi.org/10.1016/j.gloplacha.2012.10.018>. (ISSN: 0921-8181).  
412  
413 Bojinski, S., Verstraete, M., Peterson, T.C., Richter, C., Simmons, A., and Michael  
414 Zemp., 2014. The concept of essential climate variables in support of climate research,  
415 applications, and policy. American Meteorological Society. Pp.- 1431-1443.  
416 September 2014  
417  
418 Burgess, M.M., Smith, S.L., Brown, J., Romanovsky, V., Hinkel, K., 2000. Global  
419 Terrestrial Network for Permafrost (GTNet-P) permafrost monitoring contributing to  
420 global climate observations. Geological Survey of Canada, Current Research  
421 2000E14, 167.  
422 Brown, J., Hinkel, K.M and F.E. Nelson., 2000. The circumpolar active layer  
423 monitoring (CALM) program: research designs and initial results, *Polar Geography*,  
424 24 (3), 165-258.  
425  
426 De Pablo, M.A., Ramos, M., Molina. A., 2014. Thermal characterization of the active  
427 layer at the Limnopolar Lake CALM-S site on Byers Peninsula (Livingston Island),  
428 Antarctica. *Solid Earth* 5, 7216739.  
429  
430 De Pablo, M.A., Ramos, M., and Molina, A. 2016. Snow cover evolution, on 2009-  
431 2014, at the Limnopolar Lake CALM-S site on Byers Peninsula, Livingston Island,  
432 Antarctica. *Catena*, In press.  
433

434 Goyanes, G.A.,Vieira, G., Caselli, A., Mora, C., Ramos, M., De Pablo, M.A., Neves,  
435 M., Santos, F., Bernardo, I., Gilichinsky, D., Abramov, A., Batista, V., Melo, R.,  
436 Niewendam, A., Ferreira, A and Marc Oliva., 2014. REGIMEN TERMICO Y  
437 VARIABILIDAD ESPACIAL DE LA CAPA ACTIVA EN ISLA DECEPCION,  
438 ANTARTIDA. Revista de la Asociación Geológica Argentina. Pp. 112-124 Vol. 71,  
439 No 1 (2014) ISSN 1851-8249 (en línea). ISSN 1669-7316 (impreso).  
440 <http://ppct.caicyt.gov.ar/index.php/raga/issue/view/192/showToc>  
441  
442 Guglielmin, M., 2006. Ground surface temperature (GST), active layer, and  
443 permafrost monitoring in continental Antarctica. *Permafrost and Periglacial Processes*  
444 17(2): 133-143. DOI: 10.1002/ppp.553.  
445  
446 Guglielmin, M., Worland, M.R., Cannone, N., 2012. Spatial and temporal variability  
447 of ground surface temperature and active layer thickness at the margin of Maritime  
448 Antarctica Signy Island. *Geomorphology* 155, 20-33.  
449  
450 Guglielmin, M., Worland, M.R., Baio, F., Convey, P., 2014. Permafrost and snow  
451 monitoring at Rothera Point (Adelaide Island, Maritime Antarctica): Implications for  
452 rock weathering in cryotic conditions. *Geomorphology* 225:47-56 · DOI:  
453 10.1016/j.geomorph.2014.03.051  
454  
455 Hrbá ek, F., Oliva, M., Laska, K., Ruiz-Fernández, J., de Pablo, M.A., Vieira, G.,  
456 Ramos, M., and Nývlt, D. 2016. Active layer thermal regime in two climatically  
457 contrasted sites of the Antarctic Peninsula region. *Cuadernos de Investigación*  
458 *Geográfica*, In press.

459

460 Jiménez, J.J., Ramos, M., De Pablo, M.A., Molina, A., 2014. Variabilidad térmica de la  
461 capa activa, acoplada al espesor nival, en las proximidades de la BAE Juan Carlos I.  
462 Avances métodos y técnicas de estudio en el periglaciario. Gómez, A; Salvador, F;  
463 Oliva, M; Salvá, M (eds.). Publicacions i edicions de la Universitat de Barcelona.  
464 Barcelona (2014). Pp- 287-300. ISBN- 978-84-475-3830-0.

465

466 Lewkowicz, A.G and Bonnaventure, P.P., 2008. Interchangeability of mountain  
467 permafrost probability models, Northwest Canada. Permafrost and Periglac. Process.  
468 19:49-62. DOI: 10.1002/ppp.612.

469

470 Marshall, G.J., Lagun, V., Lachlan-Cope, T.A., 2002. Changes in Antarctic Peninsula  
471 tropospheric temperatures from 1956 to 1999: a synthesis of observations and  
472 reanalysis data. International Journal of Climatology 22, 2916310.

473

474 Meredith, M.P., King, J.C., 2005. Rapid climate change in the ocean west of the  
475 Antarctic Peninsula during the second half of the 20th century. Geophysical Research  
476 Letters 32, L19604.

477

478 Nelson, F.E and N.I Shiklomanov., 2010. The Circumpolar Active Layer Monitoring  
479 Networkô CALM III (200962014): long-term observations on the Climate-Active  
480 Layer-Permafrost system. In: Blanco, J.J., Ramos, M., de Pablo, M.A. (Eds.),  
481 Proceedings of II Iberian Conference of the International Permafrost Association  
482 Periglacial, Environments, Permafrost and Climate Variability. UAH, pp. 9615 (ISBN:  
483 978-84-9138-885-5).

484

485 Navarro, F.J., Jonsell, U.Y., Corcuera, M.I., Martín-Español., 2013. Decelerated mass  
486 loss of Hurd and Johnsons Glaciers. Livingston Island, Antarctic Peninsula. Journal of  
487 Glaciology, Vol. 59, No. 213, 2013 doi: 10.3189/2013JoG12J144.

488 Osmanoglu, B., Navarro, F.J., Hock, R., Braun, M and M.I. Corcuera., 2014. Surface  
489 velocity and mass balance of Livingston Island ice cap. Antarctica. The cryosphere, 8,  
490 1807-1823, doi:10.5194/tc-8-1807-2014.

491

492 Oliva, M., Hrbacek, F., Ruiz-Fernández, J., de Pablo, M.A., Ramos, M., Vieira, G.,  
493 Antoniadis, D., 2016. Active layer dynamics in three topographically distinct lake  
494 catchments in Byers Peninsula (Livingston Island, Antarctica). Catena . Accepted.

495

496 Ramos, M., Vieira, G., Gruber, S., Blanco, J.J., Hauck, C., Hidalgo, M.A., Tome, D.,  
497 Neves, M., Trindade, A., 2007. Permafrost and active layer monitoring in the Maritime  
498 Antarctic: preliminary results from CALM sites on Livingston and Deception Islands.  
499 U.S. Geological Survey and The National Academies; USGS OF-200761047, Short  
500 Research Paper 070. doi:10.3133/of2007-1047srp070.

501 Ramos, M., Vieira G., 2009. Evaluation of the ground surface enthalpy balance from  
502 bedrock shallow borehole temperatures (Livingston Island, Maritime Antarctic). The  
503 Cryosphere 3: 1336145. [www.the-cryosphere.net/3/133/2009/](http://www.the-cryosphere.net/3/133/2009/)

504

505 Ramos, M., Vieira, G., Guilichinski, D., de Pablo, M.A., 2010. Nuevas estaciones de  
506 medida del régimen térmico del permafrost en el área de Crater Lake. Isla Decepción  
507 (Antártida). Resultados preliminares. In: Blanco, J.J., Ramos, M., de Pablo, M.A.  
508 (Eds.). Proceedings of II Iberian Conference of the International Permafrost

509 Association Periglacial, environments, permafrost and climate variability. UAH, pp.  
510 936109. ISBN: 978-84-9138-885-5.  
511  
512 Ramos, M., De Pablo, M.A., Sebastian, E., Armiens, C., Gómez-Elvira, J., 2012.  
513 Temperature gradient distribution in permafrost active layer, using a prototype of the  
514 ground temperature sensor (REMS-MSL) on deception island (Antarctica). Cold  
515 Regions Science and Technology 72, 23632. ISSN: 0165-232X.  
516 DOI:10.1016/j.coldregions. 2011.10.012.  
517  
518 Smith. S., Brown, J., 2009. Assessment of the status of the development of the  
519 standards for the Terrestrial Essential Climate Variables - T7 - Permafrost and  
520 seasonally frozen ground.  
521  
522 Styszynska, A., 2004. The origin of coreless winters in the South Shetlands area  
523 (Antarctica). Polish Polar Research 25, 45666.  
524  
525 Smellie, J.L., López-Martínez, J., 2002. Introduction to the geology and  
526 geomorphology of Deception Island. In: López-Martínez,, J., Smellie, J.L., Thomson,  
527 J.W., Thomson, M.R.A. (Eds.), BAS Geomap Series. British Antarctic Survey,  
528 Cambridge, pp. 166.  
529  
530 Turner, J., Colwell, S.R., Marshall, G.J., Lachlan-Cope, T.A., Carleton, A.M., Jones,  
531 P.D., Lagun, V., Reid, P.A., Iagovkina, S., 2005. Antarctic climate change during the  
532 last 50 years. International Journal of Climatology 25, 2796294.  
533

534 Turner, J., Bindschadler, R., Convey, P., et al., 2009. Antarctic climate change and  
535 the environment. Scientific Committee on Antarctic Research. Cambridge, England.

536

537 Turner, J., Barrand, N.E., Bracegirdle, T. J., Convey, P., Hodgson, D. A., Jarvis, M.,  
538 Jenkins, A., Marsall, G., Meredith, M. P., Roscoe, H., Shanklin, J., 2013. Antarctic  
539 climate change and the environment: an update. Polar record. 1-23. DOI:  
540 <http://dx.doi.org/10.1017/S0032247413000296> (About DOI), Published online: 18  
541 April 2013.

542

543 Vieira, G., Lopez-Martinez, J., Serrano, E., Ramos, M., Gruber, S., Hauck, C., Blanco,  
544 J.J., 2008a. Geomorphological observations of permafrost and ground-ice degradation  
545 on Deception and Livingston Islands, Maritime Antarctica. In Proceedings of the 9th  
546 International Conference on Permafrost, 29 June-3 July 2008, Fairbanks, Alaska,  
547 Extended Abstracts, Vol. 1, Kane, D., Hinkel, K (eds). University of Alaska Press:  
548 Fairbanks; 183961844.

549 Vieira, G., Hauck, C., Gruber, S., Blanco, J.J., Ramos, M. 2008b. Massive Ice Detection using  
550 Electrical Tomography Resistivity. Examples from Livingston and Deception Islands,  
551 Maritime Antarctic. Proceedings of the VI Assembleia Ibérica de Geofísica, Tomar.

552

553 Vieira, G., López, J., Serrano, E., Ramos, M., Gruber, S., Hauck, C., Blanco, J.J., 2008.  
554 Geomorphological Observations of Permafrost and Ground-Ice Degradation on  
555 Deception and Livingston Islands, Maritime Antarctica. Proceedings of the Ninth  
556 International Conference on Permafrost University of Alaska Fairbanks June 29-July  
557 3. 2008. Institute of Northern Engineering. Edited by Douglas L. Kane and Kenneth  
558 M. Hinkel. Pp- 1839-1843. NICOP-2008. ISBN 978-0-980 017 9 -2-2.

559

560 Vieira, G., Bockheim, J., Guglielmin, M., Balks, M., Abramov, A., Boelhouwers, J.,  
561 Cannone, N., Ganzert, L., Gilichinsky, D.A., Gotyachkin, S., Lopez-Martinez, J.,  
562 Meiklejohn, I., Raffi, R., Ramos, M., Schaefer, C., Serrano, E., Simas, F., Sletten, R.,  
563 Wagner, D., 2010. Thermal state of permafrost and active-layer monitoring in the  
564 Antarctic: advances during the International Polar Year 2007-2009. *Permafrost and*  
565 *Periglacial Processes* 21 (2), 182-197. doi:10.1002/ppp.685 (ISSN: 1045-6740).

566

567 World Meteorological Organization., 1997. Global Climate Observing System  
568 GCOS/GTOS. Plan for terrestrial climate related observations. Version 2.0, GCOS-  
569 32, WMO/TD, No 796. UNEP/DEIA/TR97-7. WMO, Geneva, Switzerland, 130 pages.